Geomicrobiology of Acid-Sulfate-Chloride Springs in Yellowstone National Park

William P. Inskeep[1,2*] | Timothy R. McDermott[1,2*]

[1]Thermal Biology Institute, Montana State University, Bozeman MT
[2]Department of Land Resources and Environmental Sciences, Montana State University

**Corresponding Authors*
Thermal Biology Institute
PO Box 173142
Montana State University
Bozeman, MT 59717

Tel: 406.994.5077/2190 Fax: 406.994.3933 Email: binskeep@montana.edu/timmcder@montana.edu

ABSTRACT

Acid-sulfate-chloride (ASC) springs (pH~3, 65-85°C) in Norris Geyser Basin, Yellowstone National Park, contain a suite of reduced chemical species that may serve as energy sources for thermophilic chemotrophic microorganisms. The predominant dissolved ions of ASC springs include Na^+ (13-16 m*M*), Cl^- (13-16 m*M*), SO_4^{2-} (~1.4 m*M*), and H^+ (~1 mM), as well as significant concentrations of Fe^{II}, As^{III}, H_2S(aq), CH_4(aq), CO_2(aq) and H_2(aq). Aqueous chemistry, solid phase geochemistry, and temperature co-vary in the outflow channels of ASC springs and together act to establish niche opportunities for suitably adapted microorganisms. The primary objectives of our work on ASC springs are to describe and discover the adapted microorganisms that inhabit these springs, determine their metabolic strategies, and identify linkages between microbial population distribution and *in situ* geochemical processes. Our approach has combined thorough geochemical analysis of aqueous and solid phases with molecular investigations initially targeting the 16S rRNA gene. This chapter provides a review of the predominant geochemical zones of ASC springs including H_2S(aq) degassing and elemental S deposition immediately downstream of spring discharge, followed by oxidation of As^{III} and Fe^{II} to form As^{v}-rich, hydrous ferric oxide (HFO) microbial mats. The distribution of 16S rRNA sequences throughout the outflow channels of ASC springs reveals the potential importance of H_2, H_2S, S^o, As, and Fe-transforming microorganisms that are related to members of the genera *Stygiolobus*, *Caldococcus*, *Hydrogenobaculum*, *Metallosphaera*, *Thiomonas*, *Acidimicrobium*, and *Meiothermus*, as well as several novel uncultivated bacterial and archaeal clones detected in other thermal habitats. Results to date support the hypothesis that phylogenetic and functional diversity in these geothermal systems is defined by geochemical and temperature regimes throughout the outflow channels.

Key Words

arsenic
bioenergetics
chemolithotrophs
elemental sulfur
geochemistry
iron
microbial ecology
redox couples
sulfide

1.0 INTRODUCTION

Of the numerous geothermal features distributed throughout Yellowstone National Park (YNP), many are very acidic (pH<3) due to the oxidation of S in the subsurface hydrothermal system and or contact of geothermal water with buried solfataras (Fournier et al. 1992; Xu et al. 1998). Many of these acidic geothermal sites exhibit similar chemical characteristics to nonthermal acid-mine drainage generated from pyrite oxidation (Nordstrom 1982; LeBlanc et al. 1997; Morin et al. 2004); thus their thorough study and characterization has application beyond the study of microbial ecology in extreme habitats. Acidic geothermal springs in YNP represent unique environments, harboring microorganisms with physiologies specific to such habitats and that have yet to be discovered and characterized. The low pH of these environments precludes colonization by major groups of photosynthetic bacteria such as cyanobacteria, although at moderate thermophilic temperatures (40-55°C), acid-tolerant eukaryotic algae such as *Cyanidium, Galdieria,* and *Cyanidioschyzon* find near exclusive niche opportunities at pH values below 4 (Albertano et al. 2000). Consequently, primary production in many acidic thermophilic habitats is likely dominated by chemolithotrophic prokaryotes that obtain energy from the oxidation of inorganic constituents. Many acidic geothermal features also contain what would normally be considered toxic levels of various trace elements (Phelps and Buseck 1980; Stauffer et al. 1980; Langner et al. 2001; Ball et al. 2002)—including mercury (Hg), arsenic (As), boron (B), and antimony (Sb)—suggesting that many organisms adapted to such environments possess resistance mechanisms, or perhaps utilize these constituents for metabolic functions (Silver 1996; Rosen 2002; Oremland and Stolz 2003). These extreme habitats with unique chemical signatures may be analogous to early earth or non-earth environments, and serve as models for studying functional relationships among microorganisms and biogeochemical cycling (Newman and Banfield 2002).

Acid-sulfate-chloride (ASC) springs in Yellowstone are thought to arise from the mixing of chloride water with acid-sulfate water, where the ultimate source of sulfate may come from the oxidation of reduced forms of S from buried solfataras or the hydrolysis of magmatic SO_2(g) noted in Fournier et al. 1992, and Xu et al. 1998. A common ASC spring type in Norris Basin exhibits chemical signatures dominated by mM levels of Na^+, Cl^-, SO_4^{2-}, and H^+ (pH ~3), along with μM levels of Fe(II), As(III), and NH_4^+. Ratios of Cl^-/SO_4^{2-} can vary dramatically in geothermal features throughout Norris Basin; however, the springs discussed in this review exhibit consistent Cl^-/SO_4^{2-} molar ratios of ~10-12 (Langner et al. 2001). Furthermore, the concentrations of dissolved gases such as H_2S, H_2, CO_2, and CH_4 in the source waters of these springs are significantly oversaturated with respect to earth surface atmospheric conditions. Consequently, the source waters contain a suite of reduced chemical species that may serve as energy sources for diverse and novel microbial populations colonizing the outflow channels. As we will highlight below, geochemistry and temperature co-vary in these outflow channels as near super-imposable gradients originating from the spring source, and together act to establish niche opportunities for suitably adapted microorganisms.

During the last four years, one of our primary goals has been to define functional relationships among geochemical processes and the microorganisms that inhabit ASC springs of Norris Basin, YNP. These sites are the primary subject of a National Science Foundation (NSF) Microbial Observatory project focused on the discovery and characterization of chemolithoautotrophic, thermophilic microorganisms. Our approach has combined thorough geochemical analysis of aqueous and solid phases with molecular investigations that thus far have targeted the 16S rRNA gene. Our studies have revealed microbial communities that are suitably complex, yet simple enough to offer a reasonable opportunity for understanding the role of, and possible interactions among, specific microorganisms. The fundamental hypothesis of our work is that the significant phylogenetic and functional diversity in these geothermal systems is defined by geochemical and temperature regimes throughout the outflow channels. The data presented below provide a current summary of our understanding of the geomicrobiology of ASC springs in Yellowstone National Park.

2.0 METHODS AND APPROACH

2.1 Site Locations

The Hundred Springs Plain of Norris Geyser Basin (**Figure 1a**) contains several different types of ASC springs; however, our work has focused on low-discharge, acidic springs containing H_2, S(-II,0), Fe(II), and As(III) that may serve as electron donors capable of driving primary microbial production. The data summarized in this review were obtained from three ASC springs located just south of Cinder Pool (Norris Basin), and unofficially referred to as Dragon (**Figure 1b, c**), Beowulf, and Succession Springs. The YNP Thermal Inventory Numbers and coordinates of these three springs, respectively, are NHSP106 lat 44°43'54.8" N, long 110°42'39.9" W; NHSP35 lat 44°43'53.4" N, long 110°42'40.9" W; and lat 44°43 75.7 N, long 110°42 74.7 W. These springs have also been analyzed periodically for a full suite of chemical constituents by the U.S. Geological Survey as part of Yellowstone Park's geothermal discharge inventory programs (Ball et al. 2002). These springs exhibit source water temperatures ranging from 63-84°C and flow rates ranging from approximately 10-50 L/min. Flow rates have been observed to vary considerably (as much as 50%) over the last four years, similar to seasonal fluctuations of geothermal discharge documented in Norris Basin (Friedman 1994). During the last several years, aqueous and solid phase samples have been subjected to detailed chemical characterization and molecular analyses (16S rDNA sequence analysis) to identify microbial populations present as a function of distance from spring discharge. In selected locations, microbial mat samples have been used as inoculum for enrichments designed to isolate microorganisms responsible for mediating oxidation-reduction reactions *in situ*.

2.2 Aqueous Geochemistry

Aqueous samples were filtered (0.2 μm) on site, then analyzed in Montana State University's Soil Analytical Laboratory using inductively coupled plasma (ICP) spectrometry for major ions including Ca, Mg, Na, K, Si, Al, As, Fe, and B, and trace elements including Cd, Cr, Cu, Mn, Ni, Pb, Sb, Se, and Zn. Aqueous NH_4 was determined with a flow injection analyzer using the phenolate colorimetric ($A_{630\ nm}$) procedure (APHA 1998). In addition, several analyses were routinely conducted on site including: (i) Fe(II)/Fe(III) using the ferrozine method (To et al. 1999) employing a filtered (0.2 μm) sample; (ii) H_2S(aq) using the amine sulfuric acid method (APHA 1998) with unfiltered samples (to avoid rapid degassing of H_2S upon filtration); and (iii) predominant inorganic anions (F^-, Cl^-, SO_4^{2-}, NO_3^-, CO_3^{2-}, S_2O_3, AsO_4^{3-}) using ion exchange chromatography, or IC (Dionex AS16-4 mm column). Arsenate [As(V)] was determined using IC on an untreated sample within 30 minutes of sampling, and on paired samples treated with 10 M $KMnO_4$ and concentrated HCl to oxidize As(III) to As(V). The total As values determined with IC were cross-checked against total As values determined with ICP, and found to be within 10%. The amount of aqueous As(III) was calculated as the difference between As(V) and total soluble As (As_{TS}). Control samples evaluated in the laboratory confirmed efficient oxidation of As(III) using $KMnO_4$ at low pH. For samples from Dragon Spring (1999-2000), As(III) and As(V) were determined using atomic absorption spectrometry (hydride generation) on samples untreated and samples treated with Na borohydride (Langner et al. 2001). Aqueous pH and temperature values were obtained on site using a Mettler Toledo portable ion meter (MA130) equipped with a temperature probe, where pH 1.68 and 4.01 buffers were calibrated at spring temperatures.

More recent work (2003-2004) in our laboratories has also included measurements of dissolved gas species such as H_2, CH_4, and CO_2 using a portable Varian gas chromatograph (Model CP2900). In cases where dissolved gas values are referenced in this review, aqueous samples were sealed with zero headspace in 100 mL serum bottles using butyl-acetate stoppers (underwater when possible). A known volume of liquid was withdrawn and replaced with an equivalent volume of N_2(g) and the bottles incubated with intermittent shaking for 60 minutes. Preliminary analyses determined that an equilibration time of approximately 60 minutes was required for gas-water partitioning. Samples of the headspace were injected into the gas chromatograph using Ar as a carrier gas and analyzed for H_2, CH_4, CO_2, H_2S, and CO on a dual-channel detector system. Values of headspace gas concentrations were then used to calculate

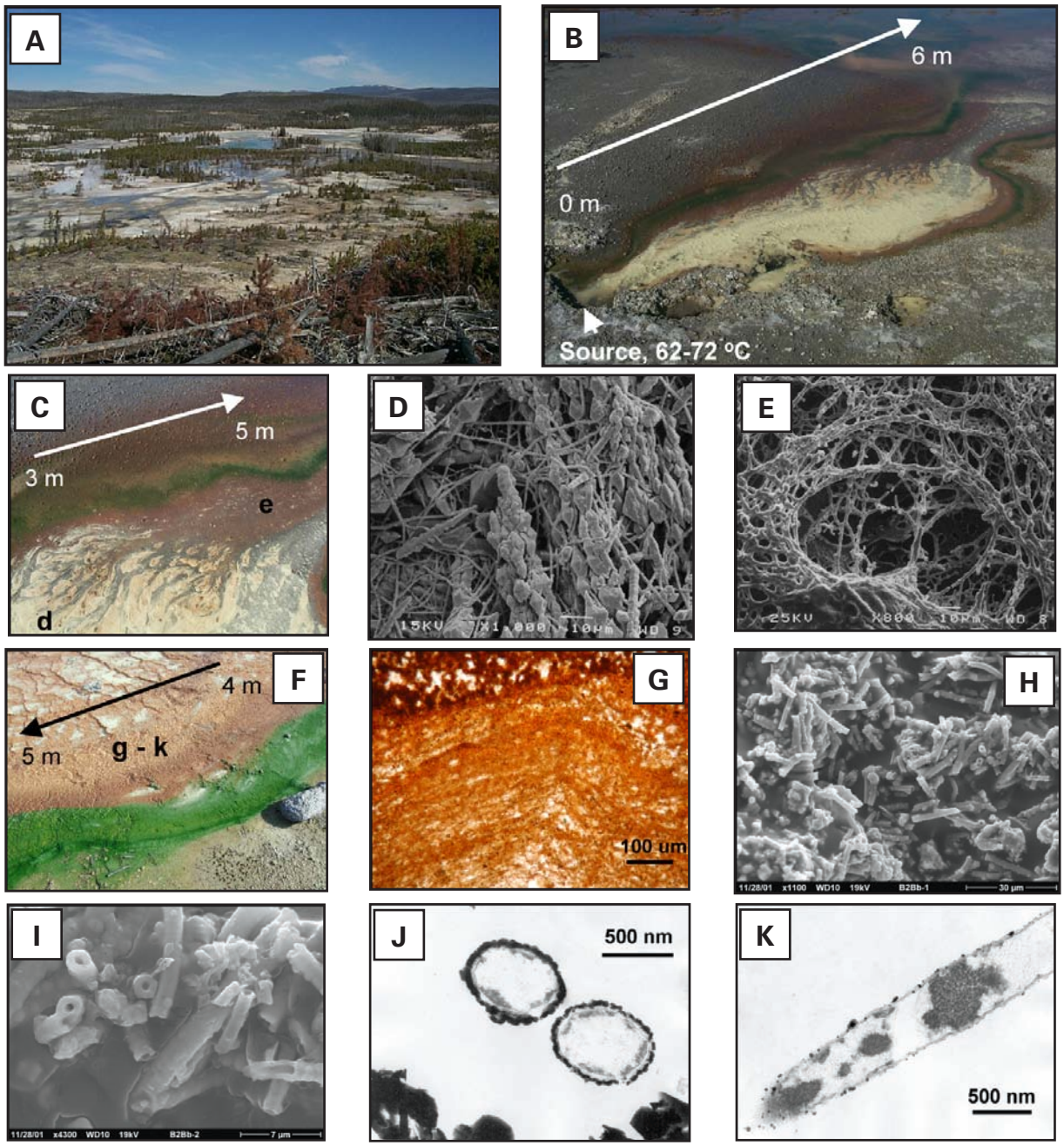

Figure 1. Photographic tour of the ASC springs *discussed in this review, scaling from a panorama of Norris Geyser Basin to the micromorphology of microorganisms found in these springs.* **A.** *One Hundred Springs Plain, looking north from Ragged Hills.* **B&C.** *Source and outflow channels of* Dragon Spring *showing prominent solid phase zonation, including the yellow S and hydrous ferric oxide (HFO) depositional zones and green bands of the eukaryotic algae* Galdieria *(temperature limit ca. 50 °C).* **D.** *Scanning electron micrograph (SEM) of yellow streamers in* **C** *reveal filamentous organisms associated with rhombohedral S.* **E.** *SEM of filamentous organisms present in Fe mats containing As-rich HFO.* **F.** *Terraced Fe mats of Beowulf Spring adjacent to eukaryotic acid-tolerant algae (presumed* Galdieria*) with an observed upper temperature limit of ~ 51 °C .* **G.** *Optical microscopic image of an HFO mat thin section from* Beowulf Spring *shows banding patterns of Fe deposition parallel to flow direction.* **H-K.** *SEM and transmission electron micrographs of HFO mats from* Beowulf Spring *show biomineralization of As(V)-HFO phases intimately associated with microbial cells.*

original dissolved gas concentrations using temperature-corrected Henry's Law constants

$$K_H = c(aq)/c(g)$$

for each gas (Amend and Shock 2001), and a mass balance equation

$$[c(aq)_{sample}\, V_L] = [c(g)_{equil}\, V_{g,eq}] + [c(aq)_{equil}\, V_{L,eq}]$$

for total dissolved gas prior to headspace equilibration where K_H = Henry's Law constant at temperature of incubation (temperature adjusted values of K_H determined from thermodynamic constants reported in Amend and Shock 2001), c = concentration in either aqueous or gas phases (mol L-1), and V = volume of liquid or gas. Concentrations of dissolved O_2 have been determined using either the Winkler method or fluorescence detection using an Rt fiber-optic fluorescence probe (Ocean Optics). The later method proved difficult due to probe instability at higher temperatures (>60°C) and need for incessant probe calibration.

2.3 Solid Phase Geochemistry

Samples of microbial mats and associated solid phases have been subjected to a compliment of analytical procedures to determine the composition, structure, and mineralogy of solid phases deposited within the outflow channels. Specifically, solid phases have been analyzed using: (i) X-ray diffraction (XRD); (ii) scanning electron microscopy and energy dispersive analysis of X-rays (SEM/EDAX); (iii) transmission electron microscopy (TEM) of glutaraldehyde-fixed and epoxy-infiltrated thin sections; (iv) X-ray absorption near edge structure (XANES) spectroscopy and extended X-ray absorption fine structure (EXAFS) spectroscopy using a synchrotron light source at the Stanford Radiation Laboratory (Inskeep et al. 2004); and (v) total chemical analysis of mat samples using a LECO furnace (for total organic C [TOC] and total organic N [TON]) and acid digestion (HNO_3-$HClO_4$-HF at 110°C). Arsenic XANES spectra of Fe-rich microbial mats were compared to model compounds including scorodite ($FeAsO_4 \cdot 2H_2O$), sodium arsenate, sodium arsenite, orpiment (As_2S_3), and arsenopyrite (FeAsS), and used to quantify As oxidation state in the samples. The EXAFS spectral region was used to determine the local coordination environment of Fe and As in the Fe-rich precipitates (Inskeep et al. 2004).

2.4 Microbial Community Analysis: DNA Extraction, Amplification and Sequencing

Microbial mat samples have also been analyzed using molecular methods to assess the distribution of 16S rDNA sequences detectable across different geochemical and temperature gradients observed in the outflow channels (Jackson et al. 2001; Inskeep et al. 2004; Macur et al. 2004). Briefly, solid phase microbial mats were sampled using sterile tools and tubes, placed on dry ice, and transported within 8 hours to a −80°C freezer. The 16S rDNA genes of bacteria and archaea present in the DNA extracts have been amplified by polymerase chain reaction (PCR)—using several primer sets, either designed for near full-length gene cloning or for sequence separation—using denaturing gradient gel electrophoresis (DGGE). One set was designed to amplify a 322 bp segment within the domain *Bacteria* using Bac1070F paired with Univ1392R, and another set used to amplify a 461 bp region within the domain *Archaea* using Arc931F and Univ1392R (Jackson et al. 2001). For DGGE-specific amplifications, the reverse primer was modified with a 40 bp gas chromatography-rich clamp to facilitate separation (Ferris et al. 1996). Details of the PCR and DGGE procedures can be found in previous publications (Ferris et al. 1996; Jackson et al. 2001). In all cases, negative control reactions (no template) were routinely performed to ensure PCR product purity. Further, PCR products were routinely examined in agarose gels to verify PCR fidelity (i.e., single amplicon of correct size). Individual DGGE bands were then purified and sequenced using the ABI Prism BigDye Terminator Cycle Sequencing Ready Reaction Kit (PerkinElmer) followed by analysis with an ABI Prism 310 capillary sequencer (PerkinElmer). Sequences were edited using Sequencher 3.1.1 software (Gene Codes Corp.) and compared with sequences found in the GenBank database using BLAST (Altschul et al. 1997). For phylogenetic analysis, cloned sequences were aligned (ClustalW; Thompson et al. 1994) and compared with the nearest neighbors identified using BLAST and with sequences representing different lines of evolutionary descent.

The work summarized here represents initial surveys on the distribution of 16S rDNA sequences observed within the outflow channels of several ASC springs, which have been used to test the hypothesis *that adapted microbial populations are distributed across gradients of temperature and aqueous chemistry*. While the initial surveys of 16S rDNA distribution in these springs do not provide a definitive functional explanation for all populations, they have (i) been extremely beneficial for developing hypotheses regarding microbially mediated redox cycling of H_2, S, As, and Fe; (ii) provided target 16S sequences for complimentary and more quantitative molecular techniques including fluorescent *in situ* hybridization (FISH) and quantitative PCR; and (iii) provided important clues for establishing relevant isolation strategies necessary for cultivation of microorganisms detected using molecular methods.

3.0 RESULTS AND DISCUSSION

3.1 Aqueous Geochemistry

3.1.1. Chemical inventory and profiles. The high-As acidic geothermal systems described here exhibit characteristics of ASC springs with chemical signatures dominated by Na^+, H^+, Cl^-, and SO_4^{2-}, and a total ionic strength of 16-20 mM (**Table 1**). More importantly, these springs contain high concentrations of reduced chemical species and dissolved gases including As(III), Fe(II), H_2, CH_4, and H_2S (**Table 1**) that represent potential energy sources for microorganisms and that serve as the main drivers of primary production in these springs. For example, three ASC geothermal springs studied in Norris Basin exhibit a fairly constant flux of µM levels of H_2S, Fe(II) and As(III), and nM levels of H_2. Significant over-saturation of geothermal source waters with respect to atmospheric levels of H_2, H_2S, CH_4 and CO_2 drives rapid degassing accompanied by oxygenation of spring waters down gradient (unpublished data). For example, concentrations of dissolved gases such as H_2S and CO_2 decline as a function of distance from spring source, and drop to below detection within several meters (**Figure 2, next page**). Simultaneously, the aqueous phase becomes increasingly oxygenated down gradient, reaching full saturation within 12 m in Succession Spring (**Figure 2**). The chemical gradients within this zone of degassing and

Table 1. Average source water chemistry of acid-sulfate-chloride geothermal springs from Norris Basin sampled periodically from 1999-2003[1].

Parameter	Unit	Acid-Sulfate-Chloride Spring		
		Dragon	Beowulf	Succession
Temperature	°C	63-70	74-80	75-84
pH		3.1	3.1	3.1
Cations				
Na	mM	16.3	13.0	12.5
K	mM	1.2	1.3	0.9
Ca	mM	0.15	0.14	0.12
Fe	µM	60	49	50-86
NH_4	µM	70	79	45
Al	µM	180	145	109
Mg	µM	10	8.2	9.4
Anions				
Cl	mM	16.0	13.8	13.3
SO_4	mM	1.3	1.5	1.3
F	mM	0.2	0.15	0.17
NO_3	µM	17	20	24
Neutral Species				
$H_4SiO_4^\circ$	mM	4.50	4.69	4.82
$H_2CO_3^\circ$	mM	4.4	1.9	1.8
$H_3BO_3^\circ$	mM	0.9	0.72	0.65
$H_3AsO_3^\circ$ {As(III)}	µM	33	24	70-80
H_2S° {S(-II)}	µM	63	79	7-80
$^2H_2^\circ$	nM	60	20-200	55
$^2CH_4^\circ$	nM	1250	1400	1650
DOC	µM	80	53	41
Ionic Strength	mM	20.0	17.5	16.5

[1] Primary data sets can be found in several recent publications: Langner et al. 2001; Inskeep et al. 2004; Macur et al. 2004.

[2] Ranges in dissolved gas concentrations represent measurements taken in 2003 (Ackerman et al., unpublished data); we have not identified the source of variation at this time, although studies are in progress to improve our understanding of dissolved gas concentrations in these springs.

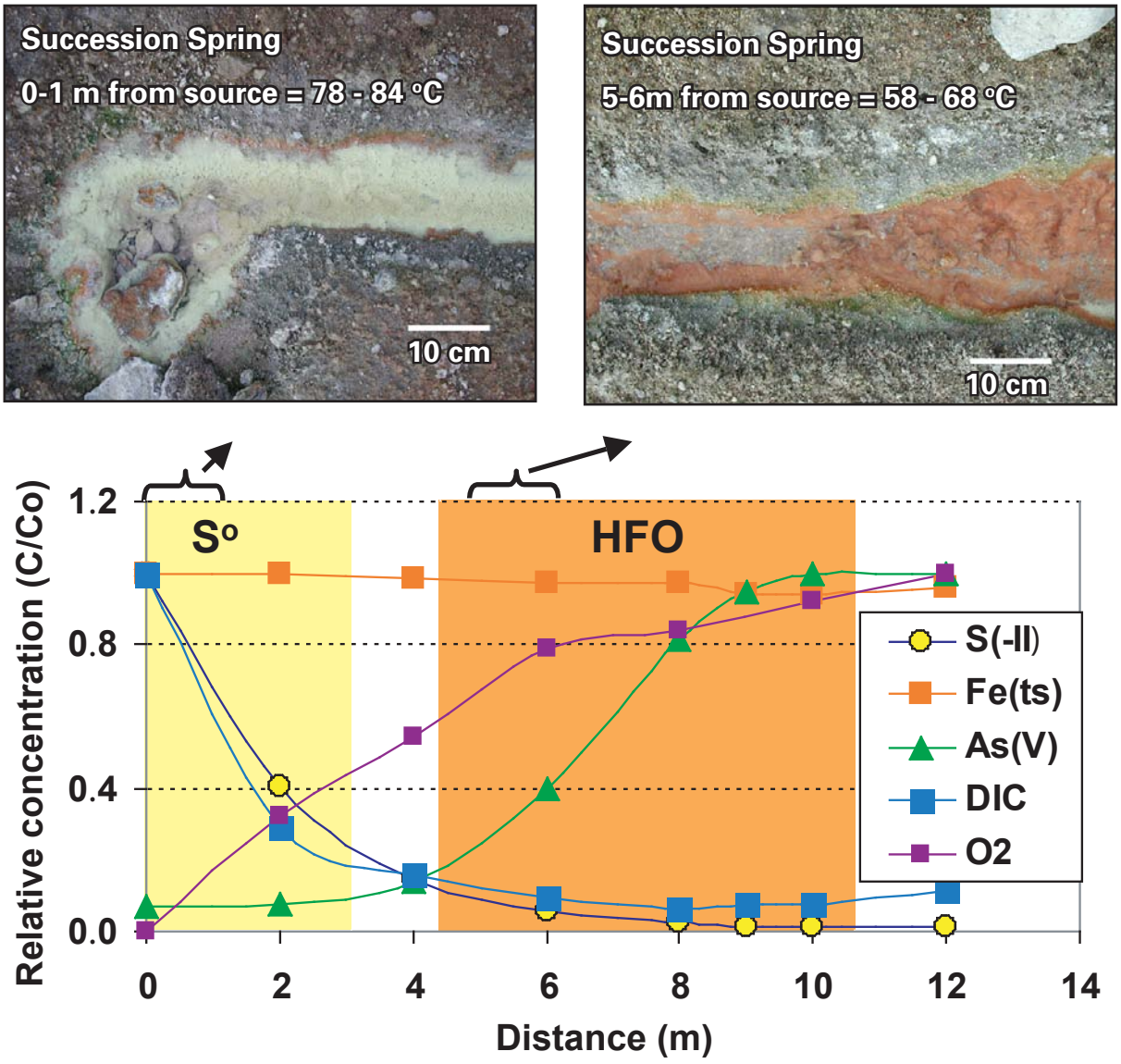

Figure 2. Photographs of two representative spring intervals (Succession Spring) *show S and hydrous ferric oxide (HFO) depositional zones and their relationship to changes in aqueous composition and temperature as a function of distance (m) down gradient from the source. The relative concentrations (C/Co) of various aqueous constituents are defined as follows: S(-II), Co = 50 µM at source; FeTS, Co = 70 µM at source; As(V), Co = 75 µM AsTS at source, which is predominantly As(III); DIC, Co= 1.8 mM at source; O_2, Co = 145 µM, corresponding to O_2 saturation at spring temperature and pressure.*

O_2-ingassing are steep, and may provide numerous habitats for microbial specialization.

The microbially mediated oxidation of aqueous As(III) commences when concentrations of H_2S(aq) drop below ~1-5 μM (**Figure 2**), and continues to increase down gradient correlating with the position of Fe-rich microbial mats (discussed below). To our knowledge, the rates of As(III) oxidation observed in these geothermal systems (first-order rate constants ranging from 1-4 min^{-1}, corresponding to approximately 0.2-0.5 μmole • min^{-1} • cm^{-3} sediment) are the fastest reported in any natural system (Langner et al. 2001; Inskeep et al. 2004; Macur et al. 2004). Consequently, the microbial communities present within these stream intervals constitute extremely efficient As(III)-oxidizing bioreactors.

For all three springs, total soluble Fe is fairly constant (±10%) throughout the outflow channel and remains predominantly as Fe(II), suggesting that the amount of Fe(II) oxidized is small relative to the flux of Fe(II) from geothermal discharge, or that Fe(III) reduction also contributes to the observed Fe species equilibria. Evidence for the oxidation of Fe(II) stems primarily from the accumulation of hydrous ferric oxide (HFO) solid phases observed in the outflow channels across temperature ranges of 48-65°C, immediately adjacent to, and just down stream of the elemental S depositional zone (**Figure 1b, c; Figure 2**). To date, we have no direct evidence that Fe(III) reduction is occurring in the HFO depositional zone; however, the limited accumulation of HFO (<1 cm depth in many regions) suggests that Fe(III) reduction may be an important component of the Fe cycle in these microbial mats.

3.1.2. Bioenergetic considerations. Chemical gradients observed in the outflow channels of ASC springs result from both abiotic and biotic processes, which define and correlate with the distribution boundaries of specific microbial populations. More specifically, the distribution of chemical species as a function of distance likely selects for, and/or results from, microbial species distribution. The relationship among microbial species distribution and chemical processes can also be evaluated in the context of chemical energy availability. The amount of energy available for microbial metabolism based on different electron donor-acceptor combinations can be estimated from free energies of reaction (ΔG_{rxn}) using the expression:

$$\Delta G_{rxn} = \Delta G^{o}_{rxn} + RT \ln Q$$

where ΔG^{o}_{rxn} = temperature-adjusted standard state reaction energy (Amend and Shock 2001), R= 8.314 $JK^{-1}mole^{-1}$, T = absolute temperature (K), and Q is the activity quotient for the reaction of interest. The activities of individual chemical species were calculated using the aqueous equilibrium model, MINTEQ (Allison et al. 1991), based on actual

Table 2. Partial list of energy-yielding (exergonic) reactions *potentially used by chemolithotrophic organisms in acid-sulfate-chloride springs of Norris Basin, YNP. Exergonic reactions (ΔGrxn <0) involving H_2, H_2S, S^o, As(III), or Fe(II) as electron donors may represent the basis for primary productivity in these acidic geothermal systems.*

Reaction[a]	ΔG_{rxn}[b]
Hydrogen [H_2(aq)]	*(kJ/ mol e^-)*
$H_2(aq) + 0.5O_2(aq) = H_2O$	-94
$H_2(aq) + 0.25NO_3^- + 0.5H^+ = 0.25NH_4^+ + 0.75H_2O$	-64
$H_2(aq) + 2Fe^{3+} = 2Fe^{2+} + 2H^+$	-63
$H_2(aq) + S^\circ = H_2S(aq)$	-16
Sulfur [H_2S(aq), S^o)]	
$H_2S(aq) + 2O_2(aq) = SO_4^{2-} + 2H^+$	-84
$H_2S(aq) + 0.5O_2(aq) = S^\circ + H_2O$	-78
$S^\circ + 1.5O_2(aq) + H_2O = SO_4^{-2} + 2H^+$	-85
$S^\circ + 6\,Fe(OH)_3(s) + 10H^+ = 6Fe^{2+} + SO_4^{-2} + 14H_2O$	-54
Arsenic and Fe	
$H_3AsO_3^\circ + 0.5O_2(aq) = H_2AsO_4^- + H^+$	-61
$H_3AsO_3^\circ + 2\,Fe(OH)_3(s) + 3H^+ = H_2AsO_4^- + 2Fe^{2+} + 5H_2O$	-28
$Fe^{2+} + 0.25O_2(aq) + H_+ = Fe^{3+} + 0.5H_2O$	-32
$Fe^{2+} + 0.25O_2(aq) + 2.5H_2O = Fe(OH)^3(s) + 2H^+$	-32
Nitrogen	
$NH_4^+ + 2O_2(aq) = NO_3^- + 2H^+ + H_2O$	-28

[a] *Reactions written in terms of predominant species at spring conditions.*

[b] *Predicted Gibbs free energy values (ΔGrxn) were based on temperature corrected equilibrium constants (Amend and Shock, 2001) and the calculated activity of each reaction constituent (Allison et al., 1991) based on measured concentrations.*

concentrations and temperatures measured in the source pools. Numerous oxidation-reduction reactions can be written for these systems, and only a subset (**Table 2, previous page**) is discussed here to illustrate the fact that there are many exergonic reactions that may be important in defining metabolic niches for specific microbial populations.

The primary electron donors in these ASC springs, including H_2(aq), H_2S(aq), S^o, Fe(II), As(III), and NH_4, all exhibit exergonic oxidation reactions with O_2(aq) or other relevant electron acceptors present in ASC springs (**Table 2**), and have been shown to support chemolithotrophic growth in various prokaryotes. As expected, O_2(aq) is always the most favorable oxidant for each electron donor, even near the spring source where O_2(aq) is at the measurement detection limit. The oxidation of H_2 with O_2 is the most thermodynamically favorable redox couple; however, oxidation reactions of H_2 with NO_3, Fe(III), or S are also exergonic. The favorable energetics of H_2 oxidation may represent an important electron donor for microorganisms in many YNP springs (Spear and Pace 2004; Spear et al. this publication). The oxidation reactions of reduced S species [H_2S(aq), S^o] are also highly exergonic under these conditions, and may be very important sources of primary productivity in the S depositional zone. The dissolved gas species such as H_2S(aq) generally decline rapidly down gradient (e.g., **Figure 2**); consequently, their importance as electron donors is likely limited to locations closer to the source. The oxidation of As(III) is also highly favorable under these conditions and may serve as an important source of electrons for certain chemolithotrophic microorganisms (Santini et al. 2000, 2002; Oremland 2004). These springs also contain abundant quantities of dissolved Fe(II), and the oxidation of Fe^{2+} to either Fe^{3+} or to $Fe(OH)_3$ (solid phase) is highly favorable in these systems (**Table 2**). Certainly, the evidence of HFO formation down gradient of S deposition (**Figure 1b, c, f; Figure 2**) suggests that organisms capable of utilizing Fe(II) are important members of these microbial communities. Finally, the oxidation of NH_4 to NO_3 is also favorable under these conditions (**Table 2**); however, we have never measured significant changes in either NH_4 or NO_3 within the outflow channels to temperatures of ~45°C. This partial list of exergonic reactions documents the potential importance of H_2, H_2S, S, As(III), and Fe(II) as electron donors for microbial growth, and illustrates the numerous electron transfer reactions that could drive primary productivity in these systems.

3.2 Solid Phase Geochemistry

3.2.1 Deposition of Elemental S. The predominant solid phase depositional patterns observed in these ASC springs include (i) a region of elemental S deposition, where H_2S(aq) concentrations range from up to 100 μM at spring source to 2-5 μM within several meters down gradient (Langner et al. 2001); and (ii) a lower temperature zone of (HFO) biomineralization that may demark a niche for organisms capable of Fe and As metabolisms (**Figure 1b, c,** and see below). The "yellow streamers" commonly observed in these ASC springs are dominated by chains of rhombohedral S intermixed with filamentous microorganisms (**Figure 1d**). The solid phase is essentially pure elemental S and exhibits an XRD pattern characteristic of crystalline S. It is not entirely clear what role microorganisms may play in the deposition of S, given that (i) the rates of H_2S oxidation to form S via thiosulfate disproportionation (Xu et al. 1998) are considered extremely rapid; and (ii) data from Succession Spring suggests that S solid phases form prior to significant colonization by microorganisms. However, the oxidation of H_2S to S with O_2 or NO_3^- as an electron acceptor is certainly exergonic under these conditions and may represent an important redox couple for microbial metabolism (**Table 2**). Perhaps more importantly, the deposition of copious amounts of S along the floor of these acid-sulfate springs provides a readily available and relatively stationary phase that serves as an important surface for microbial colonization (**Figure 1d**). Further, elemental S may serve as an electron donor or acceptor for chemolithotrophs, and may be a very important electron acceptor for chemoorganotrophs, which gain energy via the oxidation of organic C compounds (discussed below).

3.2.2 Deposition of Hydrous Ferric Oxide. Coincident with a decline in dissolved H_2S due to degassing and oxidation to S, these ASC springs consistently exhibit an abrupt geochemical transition to an As(III)- and Fe(II)-oxidizing environment several meters down gradient (**Figure 1b, c;**

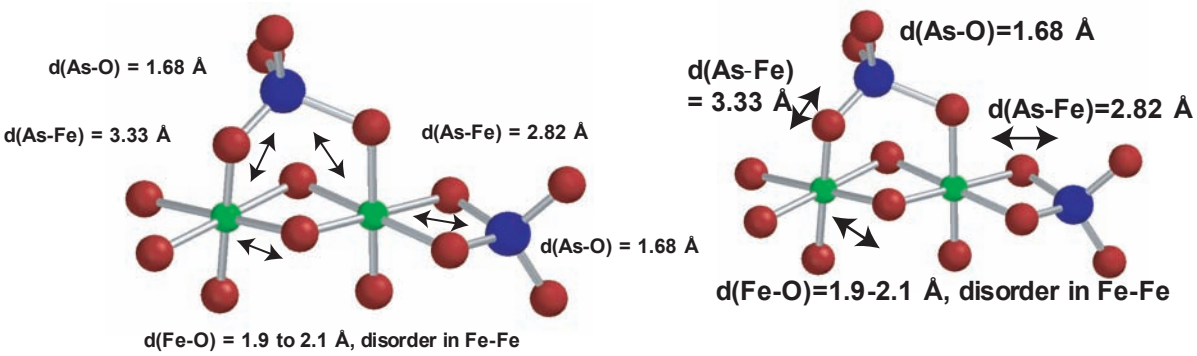

Figure 3. Chemical structure of biomineralized As(V)-HFO phase *deposited in Fe microbial mats of* Dragon, Beowulf *and* Succession Springs *as determined using x-ray absorption spectroscopy (Inskeep et al., 2004) [Red = Oxygen, Green = Fe(III), Blue = As(V)]. The spectral data support primarily the bidentate, binuclear arsenate surface complex shown with As-Fe distances of 3.33 Å. The disordered HFO phase is characterized by inconsistent Fe-O and Fe-Fe distances that would normally be observable in ordered Fe hydroxide phases.*

Figure 2). Depending on the spring, the Fe depositional zones span temperatures from 45-65°C. The rust-colored solid phases have been characterized using a complement of techniques including total chemical dissolution, XRD, SEM/EDS, transmission electron microscopy coupled with energy loss spectroscopy (TEM/EELS), XANES, and EXAFS. These studies (Langner et al. 2001; Inskeep et al. 2004) have documented that:

- The chemical composition of Fe microbial mats reveal high As contents of 0.6-0.7 moles As per mole of Fe, which are among the highest As contents found in naturally occurring As-Fe-rich deposits observed in hydrothermal vents and acid-mine drainage (LeBlanc et al. 1996; Pichler et al. 1999; Morin et al. 2004)

- The Fe solid phases are nearly entirely composed of Fe(III) and As(V) valence states as determined using XANES (Inskeep et al., 2004). Furthermore, the chemical structural information available from EXAFS confirms that As(V) is sorbed to poorly-ordered Fe(III)-OH octahedral structures (**Figure 3**). The HFO phases show typical XRD patterns for high As(V)-HFO phases (Waychunas et al. 1993,1995; Carlson et al. 2002; Rancourt et al. 2001) with two broad Bragg peaks at 0.31 and 0.15 nm, respectively (Inskeep et al. 2004). These solid phases do not show any diffraction to electrons, again indicating the poorly-ordered nature of repeating Fe-OH octahedral units, perhaps in part caused by the high sorption densities of arsenate, which likely inhibit crystal growth (Waychunas et al. 1993; Manceau 1995).

- The mechanism of formation of As(V)-HFO mats is primarily biotic, where oxidation of Fe and subsequent nucleation and growth of Fe solid phase occurs just external to, or on the cell wall of, microorganisms. Scanning and transmission electron microscopy consistently show that the As(V)-HFO phases form as sheaths and encrustations around cells, often forming 1-2 μm-thick tubules and spindles of As(V)-HFO around microbial filaments (**Figure 1h-k**). Optical microscopy also confirms the laminar appearance of these mats, where microbial filaments encrusted with HFO are the primary structural units and are consistently oriented in the direction of water flow (**Figure 1g**).

3.2.3 Summary of Acid-Sulfate-Chloride Spring Geochemistry. The predominant solid phases forming in the outflow channels of these types of ASC springs include elemental S and As(V)-HFO. Microorganisms either play a central

role in the formation of these solid phases, as is shown for the HFO mats, or may colonize surfaces of these phases for metabolic reasons. The specific relationships among aqueous chemistry, solid phase geochemistry, and microbial metabolism are the very linkages that we are interested in exploring and defining. Even in these relatively simple geochemical systems, a complex set of abiotic and biotic processes are responsible for defining the solid phases and predominant colors observed along the outflow channels (**Figure 4**).

3.3 Microbiology

Our research on the distribution of microbial populations in these ASC springs is an ongoing effort, continuing from initial molecular surveys that examined the occurrence of PCR-cloned 16S rDNA sequences as a function of distance, geochemistry, and temperature in the outflow channels of these springs (Jackson et al. 2001; Inskeep et al. 2004; Macur et al. 2004). Our findings suggest that in some cases similar patterns of sequence distribution are indeed observed among the three springs studied to date. However, there are interesting differences in the apparent populations identified among the three springs; and furthermore, there are observable differences in sequence distribution across spatial and temperature gradients within a given spring. In some cases, the differences in 16S rDNA sequences observed across the three springs appear to correlate with significant differences in source water temperature, although our current efforts are also examining the importance of chemical gradients as potential selective forces for population distribution. A summary of the predominant sequences identified in the various regions of these springs is provided in **Table 3**, along with the possible biogeochemical processes mediated by these microbial populations. The suggested biogeochemical activities of the organisms represented by these cloned sequences are inferred from known physiological traits of very phylogenetically similar organisms that have been isolated and characterized. This same information has guided our efforts to cultivate microorganisms from these springs, which can then be used to test hypotheses regarding microbial contributions to specific biogeochemical features observed *in situ* (Donohoe-Christiansen et al. 2004, and see below). These goals are part of a currently funded NSF Microbial Observatory on chemolithotrophs of acid-sulfate-chloride springs in Norris Basin.

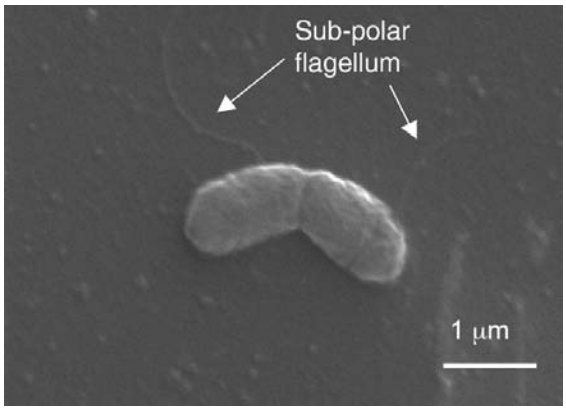

Figure 4. A scanning electron microscope image *of* Hydrogenobaculum*, strain H55, isolated from Dragon Spring in As(III)-oxidizing enrichments using H_2 as the sole energy source and CO_2 as the sole carbon source.*

3.3.1 Dragon Spring. Our first description of the diversity of microorganisms inhabiting different geochemical zones of ASC springs was performed on samples taken from the S and Fe deposition zones of Dragon Spring (Jackson et al. 2001). Clone libraries generated from PCR-amplified archaeal and bacterial 16S rDNA revealed two dominant bacterial groups in these regions, comprised primarily of *Hydrogenobaculum*- and *Desulfurella*-like organisms (**Table 3**). Of 96 bacterial clones evaluated, approximately 80% were *Hydrogenobaculum*-like and 20% *Desulfurella*-like (Jackson et al. 2001). The *Hydrogenobaculum*-like clones comprise numerous phylotypes that cluster distinctly with cultured and characterized species of *Hydrogenobaculum*, but that display as much as 4% sequence divergence. The diversity of *Hydrogenobaculum*-like sequences observed in Dragon Spring was the first evidence to suggest that these ASC springs may contain numerous highly-related (16S) *Hydrogenobaculum* organisms, perhaps specialized to different microenvironments or temperatures within the outflow channels. Other sequences detected in the HFO zone represented organisms related to *Meiothermus* and *Acidimicrobium* sp. In addition, the HFO mat samples exhibited a diverse group of archaeal clones with 16S

Table 3. **Summary of closest cultivated relatives (GenBank) of 16S rDNA sequences distributed across different solid phase depositional zones and temperatures of three different acid-sulfate-chloride geothermal springs.**

Zone	Closest Cultivated GenBank Relatives[1]	% Similarity[2]	Possible Metabolism[3] (e- donor/acceptor)	Dragon (Source = 62-64 °C)	Succession (Source = 78-84 °C)	Beowulf Spring (Source = 75-82 °C)
	Stygiolobus sp.	*96%*	*H_2 + S^o*	*Not found*	**78-84 °C, 0-1 m**	
	Thermocladium sp	*97%*	*OC + S^o*	*Not found*	**78-84 °C, 0-1 m**	
	Caldococcus sp	*99 %*	*OC + S^o*	*Not found*	**78-84 °C, 0-1 m**	
	Caldisphaera sp	*96 %*	*OC + S^o*		**65-75 °C, 2-4 m**	
	Thermocaldium sp.	*97%*	*OC + S^o*			*S zones not sampled*
S^o	*Hydrogenobaculum sp.*	*97%*	*[H_2, H_2S, S^o, and/ or As(III)] + O_2*	**58-60 °C**	**62-80 °C, 2-4 m**	
	Desulfurella sp.		*OC + [S^o, SO_4]*	**58-60 °C**	*not found*	
	Hydrogenobaculum sp.	*97%*	*[As(III), S^o] + O_2*	**50-55 °C**	**50-65 °C, 4-12 m**	*Not found*
	Desulfurella sp.	*97%*	*OC + [S^o, SO_4]*	**50-55 °C**	*not found*	*Not found*
	Acidimicrobium sp.	*-*	*Fe(II) + O_2*	**50-55 °C**	**48-55 °C, 12 m**	**58 °C**
	Metallosphaera	*98%*	*Fe(II) + O_2*	*not found*	**55-65 °C, 8 m**	**64 °C**
	Thiomonas	*98.1%*	*[Fe(II), As(III)] + O_2*	*not found*	**48-55 °C, 12 m**	**58 °C**
	Meiothermus sp.	*-*	*OC + [(Fe(III), O_2]*	**50-55 °C**	**-**	**-**
As(V)-HFO	*Marinithermus sp.*	*90.1%*	*OC + [(Fe(III), O_2]*	**-**	**52-55 °C, 12 m**	**52-55 °C**
	Multiple clones whose closest relatives are uncultured archaeal and bacterial sequences	*< 90%*	**Not possible to infer function, but all closely related clones are from thermophilic habitats**	**52 °C : Archaeal clones: A1, A6, A9, A10, A13, A14**	**60-65 °C: Archaeal clones: BG2, BG11; Bacterial clones: BG12, B14**	**58-65 °C: Archaeal clones: BG1, BG2, BG9, BG11, BG18, BG20; Bacterial clones = BG12, B14**

[1] Closest cultivated relatives of 16S rDNA sequences identified in different ASC springs as determined using Blast searches (Altschul et al., 1997). GenBank Accession numbers are provided in Jackson et al., 2001; Inskeep et al, 2004; Macur et al., 2004.

[2] In many cases, percent similarities represent averages of several closely related clones.

[3] Possible metabolisms are suggested based on knowledge of spring geochemistry and known physiology of isolates (OC = organic carbon).

rDNA sequences that were all <95% similar (averaged 89% sequence similarity across all clones) to nearest relatives in GenBank (Jackson et al. 2001).

3.3.2 Succession Spring. We have also described the spatial and temporal dynamics of microbial sequence distribution during spring colonization and mat establishment in a small ASC spring referred to as Succession Spring (**Figure 2**) that was redirected and sampled intensively for 100 days to observe relationships among geochemical transformations and microbial colonization (Macur et al. 2004). Several observations from Succession Spring confirmed patterns of 16S rDNA sequence distribution in S and Fe deposition zones; however, additional insight and interpretation was possible by correlating the appearance of microbial 16S rDNA sequences coincident with changes in aqueous and solid phase geochemistry. For example, *Hydrogenobaculum-*

like sequences were common again in the S deposition zone (**Table 3**) and were shown to correlate with the onset of As(III) oxidation two days after spring redirection (Macur et al. 2004). Several different *Hydrogenobaculum*-like sequences were consistently observed at distinct temperatures within the 55-75°C region, suggesting specialization to different temperature and/or geochemical environments. Microbial populations corresponding to the onset of HFO mat formation included *Thiomonas*-, *Metallosphaera*-, *Acidimicrobium*-, and *Marinithermus*-like organisms (**Table 3**). Although *Hydrogenobaculum-like* sequences were noted in some portions of the HFO mat, they were not associated with the onset of HFO deposition.

Source water temperatures in Succession Spring were notably higher than Dragon Spring, ranging from 78-84°C over the study period. In the high temperature regions (0-2 m), we consistently observed 16S rDNA sequences corresponding to *Stygiolobus*, *Caldococcus* and *Thermocladium*-like organisms (**Table 3**). Cultivated near-relatives of organisms represented by these sequences have all been shown to utilize S as an electron acceptor (Itoh et al. 1998), and in the case of *Stygiolobus azoricus*, the primary mode of metabolism is based on hydrogen oxidation coupled to reduction of S to form aqueous H_2S [$H^+ + S^o = H_2S(aq)$] (Segerer et al. 1991). These hyperthermophilic organisms appear to be important where S and $H_2(g)$ are both readily available, and temperatures are >75°C. This may explain the absence of such sequences in Dragon Spring, where source water temperatures were considerably lower at 63-70°C.

3.3.3 Beowulf Spring. The HFO mats of Beowulf Spring also harbor a diverse group of microbial populations, and exhibit significant shifts in community structure across changes in temperature and mat depths (Inskeep et al. 2004). Several novel (<90% similarity to cultured organisms) archaeal sequences (e.g., BG1 and BG11) were observed in HFO mats sampled at temperatures ranging from 55-65°C. Close relatives of BG1 and BG11 are uncultured clones, also recovered from thermophilic habitats (Inskeep et al. 2004). Consequently, there are several novel organisms present in the Fe mats of Beowulf Spring, and although the metabolisms of these organisms cannot be inferred with much confidence, it is likely that their metabolism is in some way coupled to Fe cycling. *Metallosphaera*-like organisms were consistently detected in warmer regions of HFO deposition (65°C), followed by *Thiomonas*-like and *Acidimicrobium*-like organisms at temperatures ranging from 55-57°C. Isolates of *Acidimicrobium* sp., *Metallosphaera* sp., and *Thiomonas* sp. are capable of utilizing Fe(II) as an electron donor (Fuchs et al. 1995; Peeples and Kelly 1995; Clark and Norris 1996), and it has been recently shown that some *Thiomonas* sp. isolated from an acid-mine drainage system are capable of oxidizing As(III), though apparently not for energy generation (Bruneel et al. 2003). As temperatures drop to 51-53°C, the Fe mats in these particular springs are often notably thinner, darker, and more brittle; the dominant DGGE bands identified in these regions were most closely related to a *Marinithermus* sp. (Sako et al. 2003), although only at 90% similarity. Future efforts will focus on more definitive identification and characterization of these organisms and their role in Fe and or As cycling.

4.0 THE IMPORTANCE OF MICROORGANISM ISOLATION IN GEOCHMICAL CYLING

Our cultivation efforts are aimed primarily at obtaining organisms that can be used to characterize and model biogeochemical reactions observed *in situ*. For example, initial 16S rDNA cloning work with mat samples from Dragon Spring suggested that *Hydrogenobaculum*-like populations were playing an important role in mediating observed As(III) oxidation. Consequently, several enrichment cultures were established that reflected the known physiology of characterized hydrogenobacula (i.e., different headspace gas combinations) and screened for their ability to oxidize As(III) (Donahoe-Christensen et al. 2004). The only cultures which oxidized As(III) contained H_2 as an energy source, microaerobic levels of oxygen (~1% O_2), and CO_2 as a sole C source. With repeated transfers followed by dilution to extinction, a pure culture of a *Hydrogenobaculum acidophilum*-like organism (strain H55; **Figure 4**) was obtained and shown to utilize H_2 as an electron donor while oxidizing As(III). In this case, the oxidation of As(III) was apparently for

detoxification purposes, as we were unable to demonstrate chemolithotrophic growth on As(III). *Hydrogenobaculum* spp. thus far isolated and characterized are known to require H_2 for growth (Shima and Suzuki 1993; Eder and Huber 2002; Donahoe-Christiansen 2004), but the oxidization of As(III) was an important finding in that it linked these populations with observed As(III) oxidation *in situ*. Further, the pH and temperature optimum for H55 (pH 3.5, 55°C) corresponded to the *in situ* conditions from where it was isolated (Donahoe-Christiansen et al. 2004). In addition, the full-length 16S rDNA sequence of H55 was a perfect match to one of the PCR-cloned sequences derived from this location.

Isolate H55 proved useful for further examining the relationship between dissolved sulfide and As(III) oxidation. Previous geochemical characterization of Dragon Spring showed that As(III) oxidation was negatively correlated with aqueous sulfide concentration (Langner et al. 2001). Clone libraries from Jackson et al. (2001) suggested that H55 was also present in the S deposition zone where dissolved sulfide concentrations are high (> 5 µM), but where As(III) oxidation is not observed *in situ* (Langner et al. 2001). To investigate the potential affects of dissolved sulfide on microbial As(III) oxidation, H55 was grown under microaerobic conditions at H_2S:As(III) ratios (60 µM:30 µM) similar to that measured *in situ* (Langner et al. 2001). Normal oxidation patterns were observed in cultures not treated with H_2S, but the presence of H_2S completely inhibited As(III) oxidation by H55 (**Figure 5**). Furthermore, the addition of an equivalent sulfide concentration as a spike midway through the experiment caused an immediate arrest of As(III) oxidation (**Figure 5**). In contrast, non-inoculated controls failed to show any As(III) oxidation nor any reduction of As(V) due to H_2S. In additional experiments where As chemical species were tracked for longer time periods, sulfide-induced As(V) reduction was slow under microaerobic conditions, requiring five days for approximately 50% reduction. Under anaerobic conditions, roughly 75% of the As(V) was reduced after only 48 hours (data not shown), approaching As(V) reduction rates observed in other studies at low pH (Rochette et al. 2000). From these results, it was concluded that the primary effect of aqueous sulfide was to act as an inhibitor of microbially mediated As(III) oxidation. This is consistent with stream measurements showing that, while

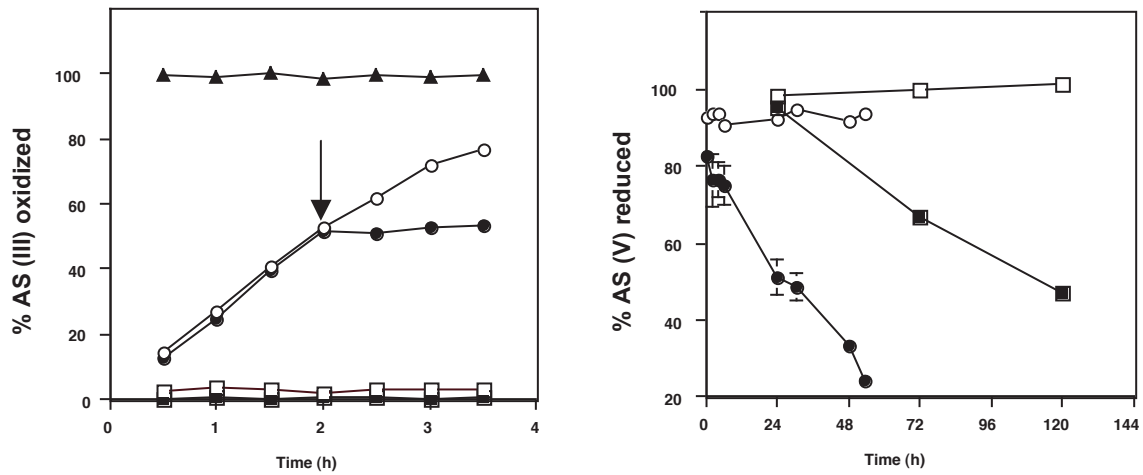

Figure 5. Influence of aqueous sulfide on As(III) oxidation by *Hydrogenobaculum* strain H55. *A. As(III) oxidation in cultures where sulfide was omitted (○), added at the beginning of the experiment (❑), or as a spike (indicated by arrow) after 2 hrs incubation (●). Additional controls included non-inoculated medium containing 30 µM As(III) (■), or 30 µM As(V) plus 60 µM aqueous sulfide (▲). B. Abiotic reduction of 30 µM As(V) by 60 µM H_2S under microaerobic (■) and anaerobic (●) conditions. Controls included microaerobic (❑) and anaerobic (○) treatments containing 30 µM As(V) but no sulfide. Error bars (where visible) depict one standard error of the mean of triplicate samples.*

As(III) oxidation is energetically favorable under spring conditions (**Table 2**), it does not commence until dissolved sulfide concentrations drop below ~5 μM (**Figure 2**).

The isolation of H55 also allowed us to examine similar questions regarding the relative importance of abiotic oxidation of As(III) via amorphous Fe(III) oxide, compared to enzyme catalyzed oxidation. The occurrence of HFO in the microbial mat used to isolate H55 is coincident with significant As(III) oxidation in the native spring, consequently, it is important to establish whether abiotic oxidation reactions with Fe(III) acting as an oxidant are comparable to those carried out by organisms such as H55. We found no effect of Fe(III) on As(III) oxidation in uninoculated controls, and there was no statistically significant influence of Fe(III) on As(III) oxidation in H55 cultures (ANOVA, P = 0.05); however, the addition of Fe(III) increased the variability in As(III) oxidation (**Figure 6**). These experiments extended beyond, but were consistent with, previous in-field assays (containing HFO microbial mats) showing that killed (formaldehyde-treated) samples failed to oxidize As(III) during short assays (~10 min). We conclude that Fe(III) in this mat does not appear to contribute significantly to measured As(III) oxidation rates relative to those catalyzed by *Hydrogenobaculum* H55 or other similarly behaving microorganisms.

5.0 COMPLEX SYSTEMS: CONCEPTUAL MODELS AND BIOLOGICAL NETWORKS

The ASC thermal springs of Norris Basin provide an interesting example of the dynamic interplay among geochemical processes and microbial species distribution (Newman and Banfield 2002; Reysenbach and Shock 2002). A suite of possible chemical and biological processes including degassing, precipitation, and oxidation-reduction reactions define the concentration profiles of reduced and oxidized chemical species throughout the spring outflow channels. Development of conceptual models describing the flux of electron donors and acceptors in ASC springs must include simultaneous consideration of purely physiochemical processes such as air-water gas exchange rates as well as the metabolic activities of microbial populations distributed throughout the outflow channels (**Figure 7**). Disappearance profiles of H_2S and CO_2 (**Figure 2**) illustrate the steep chemical gradients that may arise primarily due to the physiochemical processes controlling degassing (pH, flow rate, water surface area, turbulence, etc.). Simultaneously, the rapid microbial oxidation of As(III) provides an example of the important contribution by biota in controlling observed geochemistry. Clearly, the thermodynamic favorability of specific chemical reactions is an important consideration (i.e., **Table 2**); however, the relative rates of chemical versus biological processes will be important in defining the geochemical energy sources useful to microorganisms in ASC springs. For example, the mechanisms controlling S deposition and removal include contributions from both abiotic and biotic processes such as:

- degassing of dissolved sulfide [H_2S(aq)] to the atmosphere;
- chemical precipitation of S via oxidation of dissolved sulfide [H_2S(aq)] in the source waters;
- biomineralization of S via H_2S oxidizing microorganisms;
- formation of H_2S via microorganisms capable of utilizing S as an electron acceptor; and
- hydrologic removal of S as suspended particulates and re-deposition downstream.

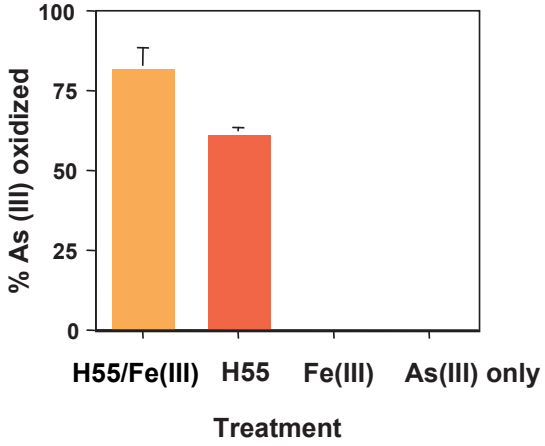

Figure 6. The effect of Fe(III) on As(III) oxidation in the presence and absence of Hydrogenobaculum strain H55. *Error bars depict one standard error of the mean of triplicate observations.*

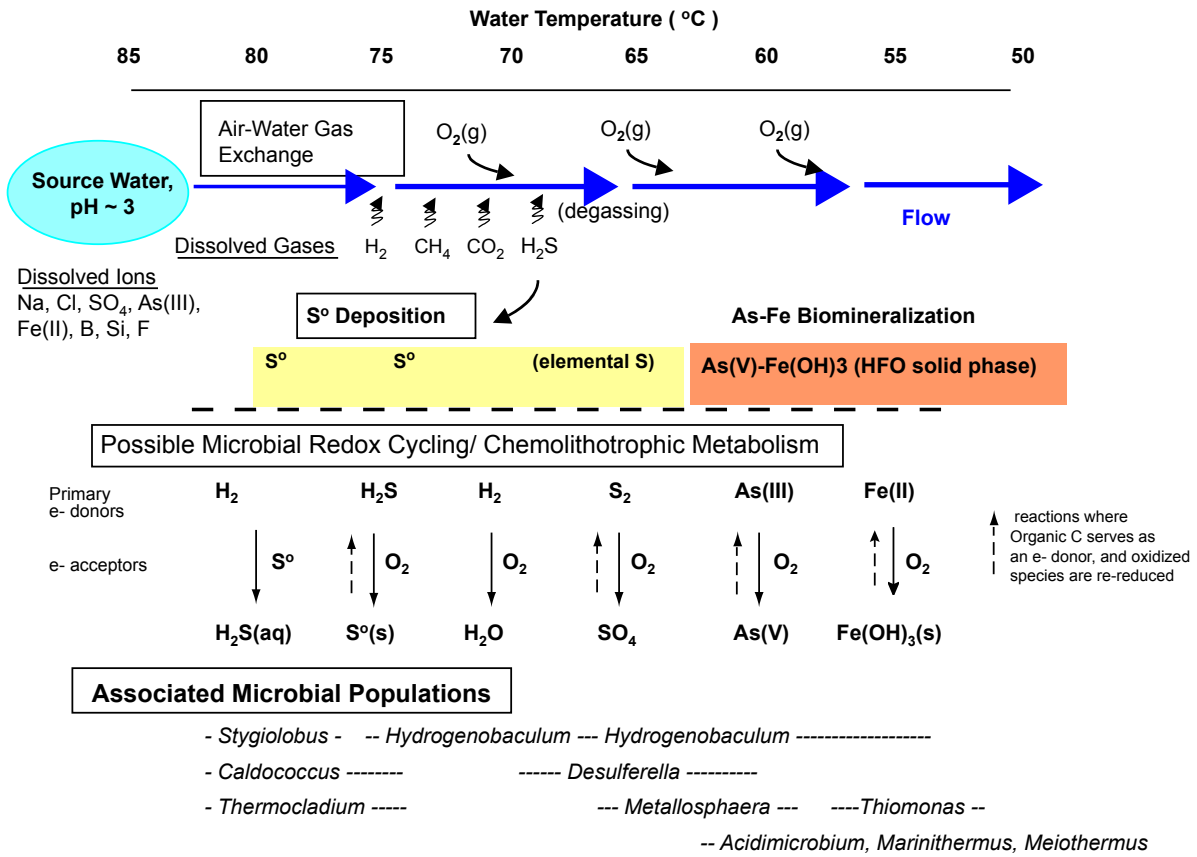

Figure 7. Diagrammatic conceptual model of major processes defining the geochemistry and associated microbial populations of acid-sulfate-chloride springs of Norris Basin, YNP.

Ultimately, the relative rates of these competitive reactions will define the amount of elemental S at any given distance from geothermal discharge. Moreover, the relative importance of each reaction may vary temporally as we have visually noted fluctuations in the amount of S deposition in springs like Dragon Spring (unpublished data).

Similarly, an exhaustive set of chemical and biological oxidation and reduction reactions of As and Fe can be envisioned in defining the deposition of As(V)-HFO (**Figure 7**). Specifically, the depth of HFO microbial mat accumulation is likely a function of the relative rates of HFO biomineralization via Fe(II)-oxidizing organisms (i.e., formation) versus the reductive dissolution of $Fe(OH)_3$-like phases via Fe(III)-reducing organisms (i.e., consumption). Abiotic, chemical precipitation rates of HFO phases in low pH, Fe(II) solutions are slow compared to the residence times in these ASC springs (Nordstrom and Southam 1997). Consequently, it appears that the rates of biomineralization are linked directly with the growth and activities of particular members of the microbial community. Several of the 16S rDNA sequences retrieved from HFO mats (**Figure 7**) represent organisms phylogenetically similar (96-98% similarity) to known Fe(II) oxidizers. However, it is highly likely that members of this community are also utilizing $Fe(OH)_3$ as an electron acceptor (Johnson et al. 2003). The deposition of HFO in these ASC springs is consistently located just downstream of the S deposition zone where there is less

than 2 μM H_2S. Consequently, the rate and location of HFO deposition is in part linked to the rate of degassing and consumption of H_2S. The extent and location of HFO deposition may also be regulated by temperature optima of relevant microorganisms responsible for Fe(II) oxidation. Finally, the dynamics between Fe(II)-oxidizing and Fe(III)-reducing populations likely play an important role in defining HFO mat thickness as a function of time and space. Current investigations are aimed at sorting through these possibilities.

6.0 SUMMARY OF CURRENT KNOWLEDGE BASE

Our initial characterization of microbial community structure in ASC springs as a function of temperature and geochemistry has revealed apparent patterns of population distribution that are consistent with the aforementioned hypotheses *that different microorganisms are adapted to specific conditions observed throughout the outflow channels*. These first-generation studies suggest that specific populations are linked with observed biogeochemical processes. Numerous novel organisms have been identified, and several are current targets of isolation efforts aimed at obtaining pure cultures that in turn will provide opportunities for defining their metabolic capabilities and specific contribution(s) to geochemical cycling. Longer term, we hope to provide a more quantitative and integrated structure-function model where the rates of important abiotic and biotic reactions are understood, and the oxidation-reduction reactions of interest are linked to the activity of specific microbial populations.

ACKNOWLEDGEMENTS

This work was supported by the Thermal Biology Institute through a grant (NAG5-8807) provided by the National Aeronautics and Space Administration (NASA), and by the National Science Foundation (NSF) Microbial Observatory program (MCB-0132022). The project was also supported by the Montana Agricultural Experiment Station (projects 911398 and 911310). We thank J. Varley and C. Hendrix, and the Yellowstone Center for Resources for permitting this work in YNP.

References

Albertano, P., C. Ciniglia, G. Pinto, and A. Pollio. 2000. The taxonomic position of *Cyanidium*, *Cyanidioschyzon*, and *Galdieria*: an update. *Hydrobiologia* 433:137-43.

Allison, J.D., D.S. Brown, and K.J. Novo-Gradac. 1991. MINTEQA2/PRODEFA2, a geochemical assessment model for environmental systems: Version 3.0 User's Manual. Environmental Research Laboratory, Office of Research and Development, USEPA, Athens, Georgia.

Altschul, S.F., T.L. Madden, A.A. Schäffer, J. Zhang, Z. Zhang, W. Miller, and D.J. Lipman. 1997. Gapped BLAST and PSI-BLAST: a new generation of protein database search programs. *Nucl Acids Res* 25:3389-3402.

Amend, J.P., and E.L. Shock. 2001. Energetics of overall metabolic reactions of thermophilic and hyperthermophilic Archaea and Bacteria. *FEMS Microbiol Rev* 25:175-243.

APHA. 1998. *Standard methods for the examination of water and wastewater*, ed. L.S. Clesceri, A.E. Greenberg, and A.D. Eaton. Washington DC: American Public Health Association.

Ball, J.W., R.B. McCleskey, D.K. Nordstrom, J.M. Holloway, and P.L. Verplanck. 2002. Water-chemistry data for selected springs, geysers, and streams in Yellowstone National Park, Wyoming 1999-2000. *US Geol Surv Open File Rep* 02-382.

Bruneel, O., J.C.Personné, C. Casiot, M. Leblanc, F. Elbaz-Poulichet, B.J. Mahler, A. Le Flèche, and P.A.D. Grimont. 2003. Mediation of arsenic oxidation by *Thiomonas* sp. in acid-mine drainage (Carnoulès, France). *J Appl Microbiol* 95:492-9.

Carlson, L., J.M. Bigham, U. Schwertmann, A. Kyek, and F. Wagner. 2002. Scavenging of As from acid mine drainage by schwertmannite and ferrihydrite: A comparison with synthetic analogues. *Environ Sci Technol* 36:1712-19.

Clark, D.A., and P.R. Norris. 1996. *Acidomicrobium ferrooxidans* gen. nov., sp. nov.: mixed-culture ferrous iron oxidation with *Sulfobacillus* species. *Microbiol* 142:785-90.

Donahoe-Christiansen, J., S. D'Imperio, C.R. Jackson, W.P. Inskeep, and T.R. McDermott. 2004 Arsenite-oxidizing *Hydrogenobaculum* strain isolated from an acid-sulfate-chloride geothermal spring in Yellowstone National Park. *Appl Environ Microbiol* 70:1865-8.

Eder, W., and R. Huber. 2002. New isolates and physiological properties of the Aquificales and description of *Thermocrinis albus* sp. nov. *Extremophiles* 6:309-18.

Ferris, M.J., G. Muyzer, and D.M. Ward. 1996. Denaturing gradient gel electrophoresis profiles of 16S rRNA-defined populations inhabiting a hot spring microbial mat community. *Appl Environ Microbiol* 62:340-6.

Fournier, R.O. 1989. Geochemistry and dynamics of the Yellowstone National Park hydrothermal system. *Ann Rev Earth Planet Sci* 17:13-53.

Friedman, I. 1994. Effect of potential geothermal development on the thermal features of Yellowstone National Park; pt 1, perspective 3; Possible effect of nearby geothermal development on Yellowstone National Park. *GSA Today* 4:297-9.

Fuchs, T., H. Huber, K. Teiner, S. Burggraf, and K.O. Stetter. 1995. *Metallosphaera prunae* sp. nov., a novel metal-mobilizing, thermoacidophilic Archaeum, isolates from a uranium mine in Germany. System. *Appl Microbiol* 18:560-6.

Gihring, T.M., G.K. Druschel, R.B. McCleskey, R.J. Hamers, and J.F. Banfield. 2001. Rapid arsenite oxidation by *Thermus aquaticus* and *Thermus thermophilus*: Field and laboratory investigations. *Environ Sci Technol* 35:3857-62.

Inskeep, W.P., R.E. Macur, G. Harrison, B.C. Bostick, and S. Fendorf. 2004. Biomineralization of As(V)-hydrous ferric oxyhydroxide mats in an acid-sulfate chloride geothermal spring of Norris Geyser Basin, Yellowstone National Park. *Geochim Cosmochim Acta* 68:3141-55.

Itoh, T., K. Suzuki, and T. Nakase. 1998. *Thermocladium modestius* gen. nov., sp. nov., a new genus of rod-shaped, extremely thermophilic crenarchaeote. *Int J Syst Bacteriol* 48:879-87.

Jackson, C.R., H.W. Langner, J. Donahoe-Christiansen, W.P. Inskeep, and T.R. McDermott. 2001. Molecular analysis of microbial community structure in an arsenite-oxidizing acidic thermal spring. *Environ Microbiol* 3:532-42.

Johnson, D.B., N. Okibe, and F.F. Roberto. 2003. Novel thermo-acidophilic bacteria isolated from geothermal sites in Yellowstone National Park: physiological and phylogenetic characteristics. *Arch Microbiol* 180:60-8.

Langner, H.W., C.R. Jackson, T.R. McDermott, and W.P. Inskeep. 2001. Rapid oxidation of arsenite in a hot spring ecosystem, Yellowstone National Park. *Environ Sci Technol* 35:3302-9.

Leblanc, M., B. Achard, D. Ben Othman, J.M. Luck, J. Bertrand-Sarfati, and J.C. Personné. 1996. Accumulation of arsenic from acidic mine waters by ferruginous bacterial accretions (stromatolites). *Appl Geochem* 11:541-54.

Macur, R.E., H.W. Langner, B.D. Kocar, and W.P. Inskeep. 2004. Linking geochemical processes with microbial community analysis: Successional dynamics in an arsenic-rich, acid-sulfate-chloride geothermal spring. *Geobiology* (in press).

Manceau, A. 1995. The mechanism of anion adsorption on Fe oxides: Evidence for the bonding of arsenate tetrahedra on free Fe(O, OH)6 edges. *Geochim Cosmochim Acta* 59:3647-53.

Morin, G., F. Juillot, C. Casiot, O. Bruneel, J.C. Personné, F. Elbaz-Poulichet, M. Leblanc, P. Ildefonse, and G. Calas. 2003. Bacterial formation of tooeleite and mixed arsenic(III) or arsenic(V) - iron (III) gels in the Carnoulès acid mine drainage, France. A XANES, XRD, and SEM study. *Environ Sci Technol* 37:1705-12.

Newman, D.K., and J.F. Banfield (2002) Geomicrobiology: How molecular-scale interactions underpin biogeochemical systems. *Science* 296:1071-7.

Nordstrom, D.K. 1982. Aqueous pyrite oxidation and the consequent formation of secondary iron minerals. In *Acid-Sulfate Weathering*, no. 10, ed. J. Kittrick, D. Fanning, and L. Hossner, 37-56. Madison, WI: Soil Science Society of America.

Nordstrom, D.K., and G. Southam. 1997. Geomicrobiology of sulfide mineral oxidation. *Rev Mineral* 35:361-90.

Oremland, R.S., and J.F. Stolz. 2003. The ecology of arsenic. *Science* 300:939-44.

Peeples, T.L., and R.M. Kelly. 1995. Bioenergetic response of the extreme thermoacidophile *Metallosphaera sedula* to thermal and nutritional stresses. *Appl Environ Microbiol* 61:2314-21.

Phelps, D., and P.R. Buseck. 1980. Distribution of soil mercury and the development of soil mercury anomalies in the Yellowstone Geothermal Area, Wyoming. *Econ Geol* 75:730-41.

Pichler, T., J. Veizer, and G.E.M. Hall. 1999. Natural input of As into a coral-reef ecosystem by hydrothermal fluids and its removal by Fe(III) oxyhydroxides. *Environ Sci Technol* 33:1373-8.

Rancourt, D.G., D. Fortin, T. Pichler, P.J. Thibault, G. Lamarche, R.V. Morris, and P.H.J. Mercier. 2001. Mineralogy of a natural As-rich hydrous ferric oxide coprecipitate formed by mixing of hydrothermal fluid and seawater: Implications regarding surface complexation and color banding in ferrihydrite deposits. *Am Mineral* 86:834-51.

Reysenbach, A.-L., and E. Shock. 2002. Merging genomes with geochemistry in hydrothermal ecosystems. *Science* 296:1077-82.

Rochette, E.A., B.C. Bostick, G. Li, and S. Fendorf. 2000. Kinetics of arsenate reduction by dissolved sulfide. *Environ Sci Technol* 34:4714-20.

Rosen, B.P. 2002. Transport and detoxification systems for transition metals, heavy metals and metalloids in eukaryotic and prokaryotic microbes. *Comp Biochem Physiol* 133:689-93.

Sako, Y, S. Nakagawa, K. Takai, and K. Horikoshi. 2003. *Marinithermus hydrothermalis* gen. nov., sp. nov., a strictly aerobic, thermophilic bacterium from a deep-sea hydrothemal vent chimney. *Int J Syst Evol Microbiol* 53:59-65.

Santini, J.M., L.I. Sly, R.D. Schnagl, and J.M. Macy. 2000. A new chemolithoautotrophic arsenite-oxidizing bacterium isolated from a gold mine: Phylogenetic, physiological, and preliminary biochemical studies. *Appl Environ Microbiol* 66:92-7.

Santini, J.M., L.I. Sly, A. Wen, D. Comrie, P. De Wulf-Durand, and J.M. Macy. 2002. New arsenite-oxidizing bacteria isolated from Australian gold mining environments-phylogenetic relationships. *Geomicrobiol J* 19:67-76.

Segerer, A.H., A. Trincone, M. Gahrtz, and K.O. Stetter. 1991. *Stygiolobus azoricus* gen. nov., sp. nov., represents a novel genus of anaerobic, extremely thermoacidophilic archaebacteria of the order Sulfolobales. *Int J Syst Bacteriol* 41:495-501.

Shima, S., and K.I. Suzuki. 1993. *Hydrogenobacter acidophilus* sp. nov., a thermoacidophilic, aerobic, hydrogen-oxidizing bacterium requiring elemental sulfur for growth. Int J Syst Bacteriol 43:703-8.

Silver, S. 1996. Bacterial resistances to toxic metal ions-a review. *Gene* 176:9-19.

Spear, J.R., and N.R. Pace. 2004. Diversity of life at the geothermal subsurface-surface interface: The Yellowstone Example. In *The Subseafloor Biosphere: American Geophysical Union Monograph*, ed. W. Wilcock W, 339-50. AGU Geophysical Monograph Series. Washington DC: American Geophysical Union.

Stauffer, R.E., E.A. Jenne, and J.W. Ball. 1980. Chemical studies of selected trace elements in hot-spring drainages of Yellowstone National Park. *US Geol Surv Prof Pap* 1044-F.

Thompson, J.D., D.G. Higgins, and T.J. Gibson. 1994. Clustal W: Improving the sensitivity of progressive multiple sequence alignment through sequence weighting, position-specific gap penalties and weight matrix choice. *Nucl Acids Res* 22:4673-80.

To, T.B., D.K. Nordstrom, K.M. Cunningham, J.W. Ball, and R.B. McCleskey. 1999. New method for the direct determination of dissolved Fe(III) concentration in acid mine waters. *Environ Sci Technol* 33:807-13.

Waychunas, G.A., Rea B.A., Fuller C.C., and J.A. Davis. 1993. Surface chemistry of ferrihydrite: Part 1. EXAFS studies of the geometry of coprecipitated and adsorbed arsenate. *Geochim Cosmochim Acta* 57:2251-69.

Waychunas, G.A., J.A. Davis, and C.C. Fuller. 1995. Geometry of sorbed arsenate on ferrihydrite and crystalline FeOOH: Re-evaluation of EXAFS results and topological factors in predicting sorbate geometry, and evidence for monodentate complexes. *Geochim Cosmochim Acta* 59:3655-61.

Wilkie, J.A., and J.G. Hering. 1998. Rapid oxidation of geothermal arsenic(III) in stream waters of the eastern Sierra Nevada. *Environ Sci Technol* 32:657-62.

Xu, Y., M.A.A. Schoonen, D.K.Nordstrom, K.M. Cunningham, and J.W.Ball. 1998. Sulfur geochemistry of hydrothermal waters in Yellowstone National Park: I. The origin of thiosulfate in hot spring waters. *Geochim Cosmochim Acta* 62:3729-43.